

## Reinterpret the heterogeneous reaction of $\alpha$ -Fe<sub>2</sub>O<sub>3</sub> and NO<sub>2</sub> with 2D-COS: The role of SDS, UV and SO<sub>2</sub>

Haojie Duan<sup>a</sup>, Hejingying Niu<sup>a,\*</sup>, Lina Gan<sup>b,\*</sup>, Xiaodi Duan<sup>a</sup>, Shuo Shi<sup>c</sup>, Li Li<sup>a</sup>

<sup>a</sup>School of Environmental & Chemical Engineering, Shanghai University, Shanghai 200444, China

<sup>b</sup>School of Environment and Architecture, University of Shanghai for Science and Technology, Shanghai 200093, China

<sup>c</sup>Shanghai Aircraft Design and Research Institute, Shanghai 201210, China



### ARTICLE INFO

#### Article history:

Received 31 May 2023

Revised 3 August 2023

Accepted 1 September 2023

Available online 3 September 2023

#### Keywords:

Heterogeneous reaction

$\alpha$ -Fe<sub>2</sub>O<sub>3</sub>

2D-COS

SDS

Aerosol

### ABSTRACT

Heterogeneous reaction of mineral aerosols and atmospheric polluting gases play an important role in atmospheric chemistry. In this study, the reactions of NO<sub>2</sub> with or without SO<sub>2</sub> mixture gas on the surface of  $\alpha$ -Fe<sub>2</sub>O<sub>3</sub> particles under dry conditions were studied. The effects of sodium dodecyl sulfate (SDS) and the heterogeneous reaction under both dark and UV irradiation conditions were investigated. The infrared spectrum analyzed by the two-dimensional correlation spectroscopy (2D-COS) was used to obtain the products formation sequences. The results showed that UV irradiation can promote the production of nitrate. The 2D-COS analysis indicated SDS changed the sequence order of nitrate and nitrite species during reactions. In oxidation conditions, the final product of heterogeneous reaction of NO<sub>2</sub> and  $\alpha$ -Fe<sub>2</sub>O<sub>3</sub> was monodentate nitrate. Only the heterogenous reaction of NO<sub>2</sub> and  $\alpha$ -Fe<sub>2</sub>O<sub>3</sub> containing SDS (FOS) without UV light, the final product was bidentate nitrate. SDS was the catalysis agent supply and photoresist to the system. With surface active compounds, the environmental lifetime of heterogeneous reactions between trace gases and aerosols extends. Surfactants, ultraviolet light, and the types of gases involved in the reaction all have complex effects on the aerosol aging process. This study provided a reference for subsequent heterogeneous reaction studies and the formation of aerosols.

© 2024 Published by Elsevier B.V. on behalf of Chinese Chemical Society and Institute of Materia Medica, Chinese Academy of Medical Sciences.

As one of the major tropospheric aerosols, mineral aerosols can be transported over long distances and interact with atmospheric pollutants (such as NO<sub>2</sub> and SO<sub>2</sub>) during transmission. With a reaction surface provided mineral aerosols, heterogeneous reactions occur between mineral aerosols and gases, which change the composition and surface properties of mineral dust [1], and further affect climate and human health [2–4]. Trivalent iron is an important component of the Earth's crust [5], due to wind and volcanic activity [6], it is easily transferred to the atmosphere in the form of aerosols of iron-containing mineral dust [7]. In addition,  $\alpha$ -Fe<sub>2</sub>O<sub>3</sub> is a typical component of mineral dust and also has thermodynamic stability and photocatalysis properties [8]. During UV light irradiation,  $\alpha$ -Fe<sub>2</sub>O<sub>3</sub> is one pathway of atmospheric gases sink. In this study, iron oxide was chosen as the model oxide.

NO<sub>2</sub> and SO<sub>2</sub> are important pollution gases in atmosphere, they are precursors of nitrate and sulfate. Heterogeneous reactions of mineral aerosols with acidic gases play a crucial role during the sink of acidic gases [9]. In previous studies, nitrate amount on

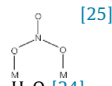
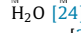
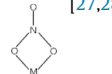
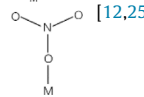
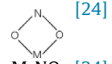
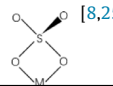
goethite is higher than that on hematite and magnetite [10]. For sulfate series, the products on the surface of  $\alpha$ -Fe<sub>2</sub>O<sub>3</sub>,  $\alpha$ -FeOOH and Fe<sub>3</sub>O<sub>4</sub> particles are mainly bidentate sulfate. By contrast, on the surface of  $\gamma$ -Fe<sub>2</sub>O<sub>3</sub> particles single-tooth Fe(III)-sulfate complex was yielded [11]. A synergistic effect was reported from the heterogeneous reaction of NO<sub>2</sub> and SO<sub>2</sub> on  $\gamma$ -Al<sub>2</sub>O<sub>3</sub> particles. NO<sub>2</sub> can act as an oxidant to promote the oxidation of SO<sub>2</sub> to sulfates [12]. In this paper, the heterogeneous reaction of NO<sub>2</sub>/SO<sub>2</sub> with Fe<sub>2</sub>O<sub>3</sub> was studied, and the effect of light and surface active constituent on the reaction were also considered with two-dimensional correlation spectroscopy (2D-COS) analysis. 2D-COS is a technique that plots spectral intensity as a function of two independent spectral variables (i.e., frequency or wavelength) [13–15]. With these 2D spectra, a simplification of complex spectra consisting of many overlapping bands or bands can be obtained. It has become an important tool for analysis for Raman with IR spectra, Raman with FTIR spectra, Ultraviolet-visible with fluorescence spectra [16–18].

Surfactant usually appears on the surface of atmospheric aerosol particles, in the form of a single layer, sheet island, or thick adsorption film [19]. The surface active compounds can enhance cloud condensation nuclei (CCN) activity in the atmosphere by reducing the surface tension or extend the lifetime of molecules

\* Corresponding authors.

E-mail addresses: [niuhyj@shu.edu.cn](mailto:niuhyj@shu.edu.cn) (H. Niu), [lngan@usst.edu.cn](mailto:lngan@usst.edu.cn) (L. Gan).

**Table 1**  
Main absorption bands in this study.

Wavenumber (cm <sup>-1</sup> )	Surface species	Vibrational mode	Representation
1662	Bridging nitrate or carbonyl	$\nu_3$ [24]	 [25]
1630	Water	$\delta(\text{HOH})$ [25]	 [24]
1594, 1285	Bidentate nitrate	1594: $\nu_3$ high [26] 1285: $\nu_3$ low [26]	 [27,28]
1574, 1493	Monodentate nitrate	1574: $\nu_3$ (high) [29] 1493: $\nu_3$ [24]	 [12,25]
1462, 1203	Chelated nitro species		 [24]
1401	Nitro compounds	$\nu_3$ [24]	M-NO <sub>2</sub> [24]
1388	Free nitrate anion	$\nu_3$ [24]	NO <sub>3</sub> <sup>-</sup> [30]
1365, 1355-1335	Water-solvated nitrate		NO <sub>3</sub> <sup>-</sup> (aq) [25,31]
1267	Nitrite		NO <sub>2</sub> <sup>-</sup> [30]
1280-1260	Free sulfate		SO <sub>4</sub> <sup>2-</sup> [8]
1151	Bidentate sulfate		 [8,25]

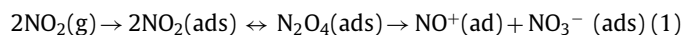
in the bulk [19,20]. With surface active organics bounding on the surface of an atmospheric particle, the heterogeneous chemistry among radicals and aerosols is modified and radical oxidation timescale is shortened [21]. Sodium dodecyl sulfate (SDS) is an anionic, nontoxic surfactant, it is often used as a surrogate for soluble atmospheric surfactants [22]. In this study, SDS was selected as a model surfactant to research its effects to the heterogeneous reaction between acid gases and photocatalytic aerosol particle.

In this paper, 2D-COS was used to analyze the heterogeneous reactions of NO<sub>2</sub>, SO<sub>2</sub> and  $\alpha$ -Fe<sub>2</sub>O<sub>3</sub> under different conditions, and the effects of UV light, surfactant SDS and the different gases involved in the reaction were investigated. The analysis process of 2D-COS was shown in Supporting information (experiment section 4). The sequence order of nitrate and nitrite species was affected by the addition of SDS, reaction environment and other gases. As a model surface active compound of this study, SDS's sulfate tail provides sulfate for the aerosol. With the sacrificing of C-H bond from SDS, the bond was photocatalyzed to carbonyl group to protect the aerosol. With 2D-COS, the heterogeneous reactions of trace gases (NO<sub>2</sub> and SO<sub>2</sub>) with  $\alpha$ -Fe<sub>2</sub>O<sub>3</sub> or  $\alpha$ -Fe<sub>2</sub>O<sub>3</sub> containing SDS (FOS) were reinterpreted. It helped to offer deep analysis to the reaction process.

The crystallinity and phase of the Fe<sub>2</sub>O<sub>3</sub> nanocomposite were identified using XRD analysis as seen in Fig. S1 (Supporting information). The pattern of Fe<sub>2</sub>O<sub>3</sub> nanoparticles displays the core  $\alpha$ -Fe<sub>2</sub>O<sub>3</sub> feature peaks [23]. Based on the XRD card, the type of Fe<sub>2</sub>O<sub>3</sub> was  $\alpha$ -Fe<sub>2</sub>O<sub>3</sub>. In this paper, all experiments spectral bands and their corresponding vibration modes in this study were shown in Table 1 [8,12,24-31].

The infrared spectra of NO<sub>2</sub> on  $\alpha$ -Fe<sub>2</sub>O<sub>3</sub> particles results were shown in Fig. S2 (Supporting information). The weak band at 1630 cm<sup>-1</sup> was attributed to water [24]. The bands at 1594 and 1285 cm<sup>-1</sup> were assigned to bidentate nitrates [27,28]. The band at 1267 cm<sup>-1</sup> was belonged to nitrite [30]. With the increase of exposure time, nitrite was converted to nitrate [30]. It indicated that nitrite was an intermediate product of the reaction [27,31]. In addition, from Fig. S2 that the band at 1267 cm<sup>-1</sup> vanished quickly when UV light was applied to the system. This result suggested that UV light promoted the transformation from nitrite to nitrate [32]. The bands at 1574, 1388, 1355 and 1336 cm<sup>-1</sup> attributed to nitrate, corresponding to monodentate nitrate, free nitrate anion and water-solvated nitrate, respectively [25,30,31]. Whether under

dark condition or with UV irradiation, the main product of the heterogeneous reaction of NO<sub>2</sub> on  $\alpha$ -Fe<sub>2</sub>O<sub>3</sub> was nitrate. This was consistent with previous findings [10,33]. However, previous research did not interpret further. Therefore, 2D-COS was used to further analyze the processes. The red and blue color indicated positive and negative correlation, respectively. As shown in Fig. S3a (Supporting information), the synchronous map under dark conditions had two main autocorrelation peaks of 1467 and 1285 cm<sup>-1</sup> along the diagonal line. Therefore, the chelated nitro species simultaneously changed with bidentate nitrate, indicating that nitrate was the main product. The asynchronous map revealed the sequential changes in several new bands (Fig. S3b in Supporting information): 1370, 1355, 1321 and 1202 cm<sup>-1</sup>. The order of the occurrence of the analysis and the observed bands was shown in Table S1 (Supporting information). It could be concluded that reaction time responses for products generally occurred in orders of chelated nitro species → water solvated nitrate → bidentate nitrates → monodentate nitrate. The gas-phase NO<sub>2</sub> was adsorbed on the surface of  $\alpha$ -Fe<sub>2</sub>O<sub>3</sub> particles to form adsorbed NO<sub>2</sub>, and then disproportionation occurred as shown in Eq. 1 [34]:



Chelated nitro species were first formed [26,34]. Then NO<sub>2</sub> interacted with adsorbed water to form water-solvated nitrate. With the continuous addition of NO<sub>2</sub>, bidentate nitrate and monodentate nitrate yielded successively [26,34]. Compared with the dark condition, three new bands were observed in the synchronous map with UV irradiation: 1389, 1365 and 1335 cm<sup>-1</sup>, shown in Fig. S3c (Supporting information). According to Fig. S3d and Table S2 (Supporting information), the sequential order for bands change was: chelated nitro species → free nitrate anion → water solvated nitrate → bidentate nitrate → monodentate nitrate. Compared with the dark condition, nitrate species (free nitric acid anion) was observed with UV irradiation. The order of free nitric acid anion was after chelated nitro species and before aqueous solvated nitrate. From previous researches, the main product of NO<sub>2</sub> on the surface of  $\alpha$ -Fe<sub>2</sub>O<sub>3</sub> particles was nitrate with or without UV irradiation [10,33]. In this study, the monodentate nitrate was the final formed functional group during NO<sub>2</sub> reacted with  $\alpha$ -Fe<sub>2</sub>O<sub>3</sub> with dark or UV irradiation condition. UV light had an obvious promoting effect on the generation of nitrate (Fig. S2) [32].

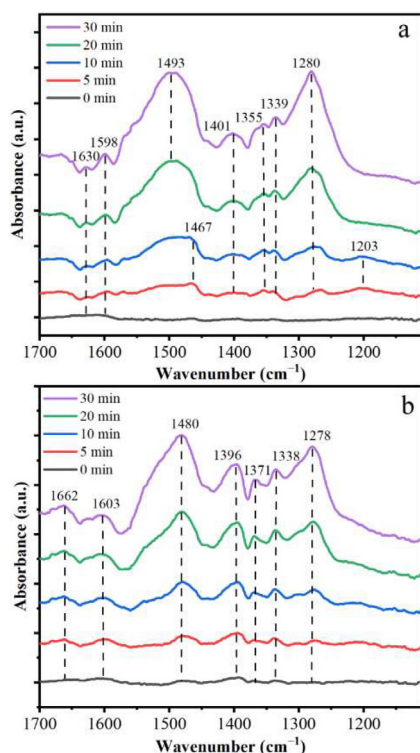


**Fig. 1.** Infrared spectra of heterogeneous reactions of  $\text{NO}_2$  on FOS particles over time: (a) Dark condition, (b) UV condition.

In addition to the heterogeneous reaction involving  $\text{NO}_2$ , the effects of SDS to the heterogeneous process were further investigated (Fig. 1). And at the beginning, two weak bands ( $1203$  and  $1467\text{ cm}^{-1}$ ) belonging to chelated nitro species formed first and disappeared after exposure to  $\text{NO}_2$  for about 10 min. In addition, the band at  $1202\text{ cm}^{-1}$  was not observed in FOS compared to the  $\text{NO}_2$  alone on the surface of  $\alpha\text{-Fe}_2\text{O}_3$  after 30 min reaction (Fig. S4 in Supporting information). Besides, the band at  $1467\text{ cm}^{-1}$  shifted to  $1493\text{ cm}^{-1}$ , i.e., chelated nitro species was converted to monodentate nitrate after adding SDS [25]. These results indicated that SDS promoted the transformation of chelated nitro species to other nitrate species comparing to the particle without SDS. The band intensity at  $1401\text{ cm}^{-1}$  which attributed to nitro compounds increased with time [24]. That suggested SDS could be beneficial to the formation of nitro compounds. The tail of SDS structure is sulfate, which adsorbs on  $\alpha\text{-Fe}_2\text{O}_3$  particles and promotes the reaction from gas phase  $\text{NO}_2$  to nitrate species [35]. On the other hand, with UV light, the monodentate nitrate band at  $1573\text{ cm}^{-1}$  disappeared on FOS comparing to  $\alpha\text{-Fe}_2\text{O}_3$  group (Fig. S4). UV irradiation inhibited the formation of chelated nitro species (Fig. 1b). Compared to heterogeneous reaction without SDS (Fig. S4), a new band at  $1662\text{ cm}^{-1}$ , which was assigned to bridging nitrate or carbonyl was observed [25,36]. The results indicated part of C-H from SDS was photocatalyzed by  $\alpha\text{-Fe}_2\text{O}_3$ . The intensity of nitrate bands at  $1662$  and  $1396\text{ cm}^{-1}$  assigned to nitrate increased. Compared with the heterogeneous reaction involving only gas [9], the addition of additives made the whole reaction process more complicated, which not only changed the types of products but also changed the generation sequence among products species.

From Figs. 2a and b, there were two autocorrelation bands of  $1491$  and  $1281\text{ cm}^{-1}$  under dark and three autocorrelation bands of  $1500$ ,  $1392$  and  $1280\text{ cm}^{-1}$  under UV conditions, respectively. Moreover, the band intensities of  $1491\text{ cm}^{-1}$  and  $1281\text{ cm}^{-1}$  were large, indicating that their sensitivity was high. The main product of the two reaction conditions was nitrate. The asynchronous map under dark condition had several new bands (Fig. 2c):  $1637$ ,  $1466$ ,

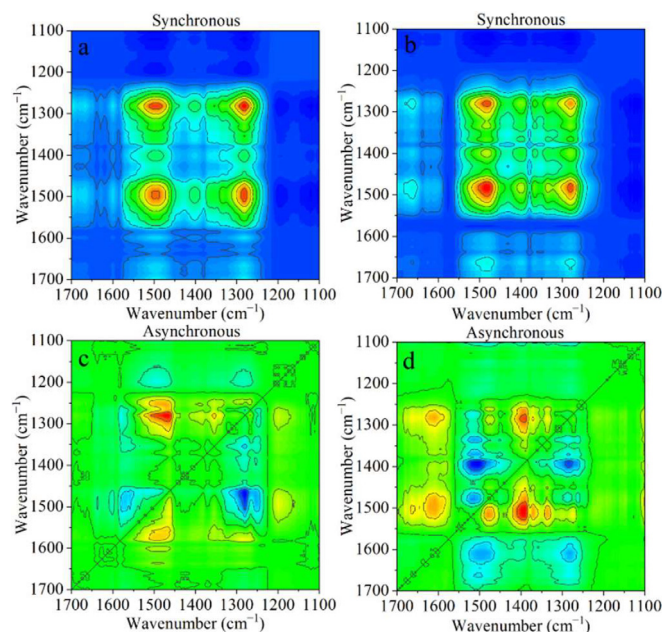


**Fig. 2.** 2D-COS spectrum of  $\text{NO}_2$  with FOS under dark and UV light: (a) Synchronous and (c) asynchronous mappings under dark condition; (b) Synchronous and (d) asynchronous mappings under UV condition.

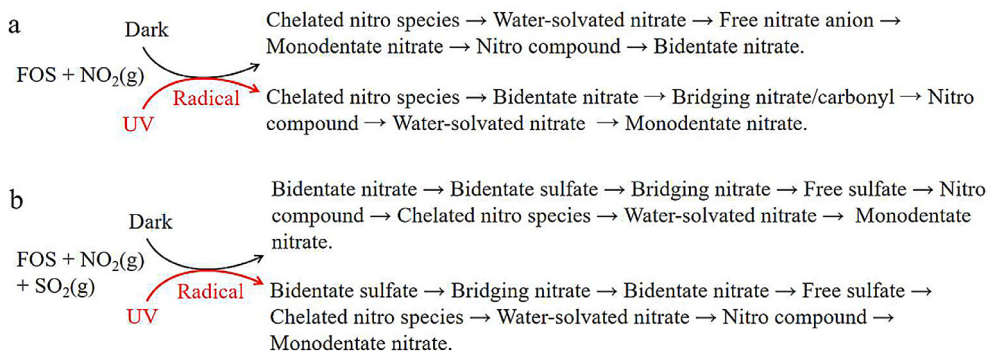
$1385$ ,  $1353$  and  $1202\text{ cm}^{-1}$ . According the analysis results demonstrated in Table 2 and Table S3 (Supporting information), the order of occurrence of bands under dark and UV irradiation conditions is shown in Scheme 1a.

According to the asynchronous map (Figs. 2c and d), UV irradiation had significant effect to the sequence of functional groups. From Scheme 1a, the chelated nitro species formed first to both dark and UV condition, this was consistent with the sample without SDS. However, to the dark experiment, bidentate nitrate and monodentate nitrate were the last functional group yielded for the FOS sample and  $\alpha\text{-Fe}_2\text{O}_3$  particles, respectively. SDS supplied additional electron to the particles and the nitrate structure on the FOS surface was bidentate [37]. With UV light irradiation, the process of FOS with  $\text{NO}_2$  was more complex. Compared to the sample without SDS, the sequence bidentate nitrate and water-solved nitrate was switched. Other nitrate species, such as bridging nitrate and nitro compound were generated. The last nitrate species (monodentate) was the same as reaction product on  $\alpha\text{-Fe}_2\text{O}_3$  particles. This may due to the photocatalysis process induced electron and hole on its surface. On the other hand, the electron was also from SDS. The complex relationship between the two parts created this phenomenon. For all samples contained SDS with UV light, the final product in the heterogeneous reaction between  $\text{NO}_2$  and FOS was monodentate (Scheme 1b). From Fig. S5 (Supporting information), the integrated area reparented the nitrate and nitrite amount. The products accumulation processes of the four experiments did not have significant difference. According to Fig. S6 (Supporting information), with UV irradiation, the intensity of C-H band ( $2977\text{ cm}^{-1}$ ) was significant comparing to its in dark condition. It suggested the SDS absorption status on the  $\alpha\text{-Fe}_2\text{O}_3$  particle was oblique with UV irradiation. This phenomenon was not observed on FOS in dark. In previous study, SDS demonstrated photoresist properties during the UV inducing oxidation [38]. In this study, with the C=O generated, energy from UV light was consumed. It extended the environmental lifetime of heterogeneous reactions between trace gases and aerosols.

The  $\text{NO}_2$  and  $\text{SO}_2$  mixture reacted with  $\alpha\text{-Fe}_2\text{O}_3$  and its infrared spectra was shown in Fig. S7 (Supporting information). Both

**Table 2**  
Band symbol relationship between synchronous and asynchronous mappings of NO<sub>2</sub> with FOS under dark condition.

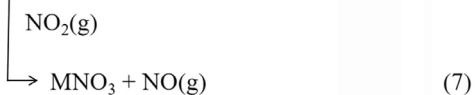
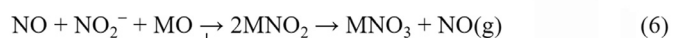
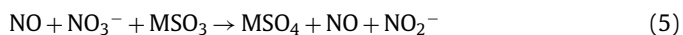
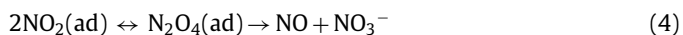
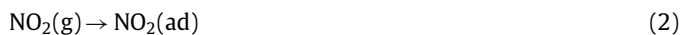
Position (cm <sup>-1</sup> )	Sign							
	1637	1491	1466	1403	1385	1353	1281	1202
1637	+	+(-)	+(-)	+(-)	+(-)	+(-)	+(-)	+(-)
1491			+(-)	+(+)	+	+	+	+
1466				+(+)	+	+	+	+
1403					+(-)	+	+	+
1385						+(-)	+	+
1353							+	+
1281								+
1202								+
Result	1202→1466→1353→1385→1491→1403→1281→1637							



**Scheme 1.** The sequential order of bands of heterogeneous reaction (a) NO<sub>2</sub> with FOS and (b) NO<sub>2</sub> and SO<sub>2</sub> with FOS under dark and UV irradiations.

in dark and UV irradiation conditions, two bands appeared at 1151 cm<sup>-1</sup> and 1266 cm<sup>-1</sup>, which were attributed to bidentate sulfate and free sulfate, respectively [8,25]. A band 1667 cm<sup>-1</sup> was observed after 10 min reaction (Fig. S7b), which was attributed to bridging nitrate [36]. The main products of this heterogeneous reaction process were sulfate and nitrate. In this study, the band assigned to nitrite was not observed, which indicated the synergistic effects of NO<sub>2</sub> and SO<sub>2</sub>.

The 2D-COS was shown in Fig. S8 (Supporting information), and the synchronous map had one autocorrelation band (Fig. S8a): 1277 cm<sup>-1</sup>, indicating that the main product was sulfate. The asynchronous map showed several bands (1599, 1577, 1459, 1396, 1377, 1330, 1280, 1268 and 1156 cm<sup>-1</sup>) as shown in Fig. S8b. The main reaction mechanism of NO<sub>2</sub> and SO<sub>2</sub> may be as follows [25,39,40]:



where M and MO represent the surface metal sites and surface reactive oxygen sites, respectively.

According to the analysis in Table S4 (Supporting information), the sequential order for the band change is shown in Fig. S9 (Supporting information).

The synchronous map under UV radiation had only two autocorrelation bands: 1504 and 1267 cm<sup>-1</sup>, which showed the strongest and most sensitive sulfate bands (Fig. S8c). Multiple cross bands appeared in the asynchronous graph (Fig. S8d). The analysis of Table S5 (Supporting information) showed that the bands followed a certain sequence, *i.e.*, Fig. S9 (Supporting information). The main products under dark and UV irradiation were sulfate and nitrate. After introduction of UV light, not only the sequence of different nitrate species was changed, but also the nitrate species were changed. The nitro compounds formed in the dark, which was not yielded with UV irradiation. The sequence of sulfate species for UV or dark experiment was the same, from the bidentate sulfate to free sulfate. For the UV group, water-solvated nitrate was the final step of reactions. Previous studies reported there was a synergistic interaction between NO<sub>2</sub> and SO<sub>2</sub> [36], with 2D-COS the process could be re-elucidated. From Figs. S10a and b (Supporting information), in dark group, the original products were accumulated in the first 10 min and generated dramatically. By contrast, the products of UV group linearly increased from the beginning.

From the two groups experiments results (Fig. S11 in Supporting information), the main heterogeneous reaction products of NO<sub>2</sub> and SO<sub>2</sub> with FOS were nitrates and sulfates. Compared to the sample without SDS (Fig. S12 in Supporting information), the band 1667 cm<sup>-1</sup> assigned to bridging nitrate was formed. The bands represented nitrate, nitrite and sulfate species (1616–1118 cm<sup>-1</sup>) were demonstrated in Figs. S10c and d. The integrated area continuously increased with time both in dark and UV conditions. The amount of dark group retarded after 20 min. In contrast, in the irradiated groups, the integrated area and the products increased during irradiation time.

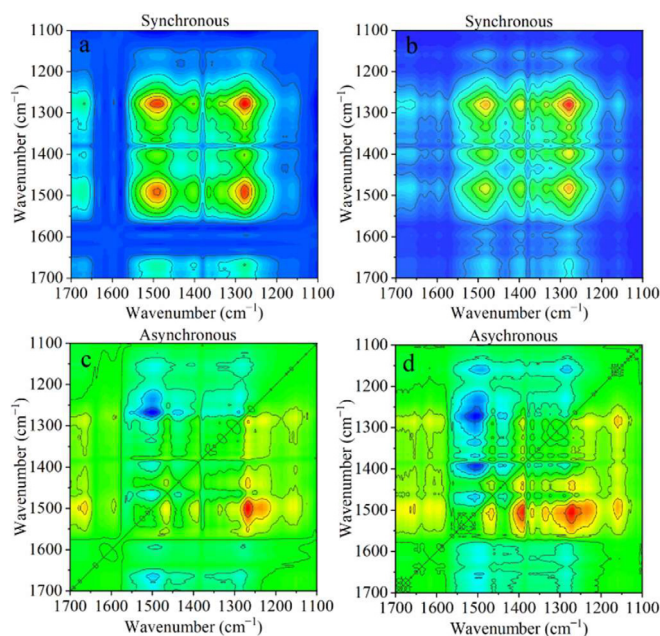


**Fig. 3.** 2D-COS spectrum of NO<sub>2</sub> and SO<sub>2</sub> with FOS under dark and UV light: (a) Synchronous and (c) asynchronous mappings under dark condition; (b) Synchronous and (d) asynchronous mappings under UV condition.

The 2D-COS showed that the synchronous map had the same autocorrelation bands (Figs. 3a and b): 1483, 1397 and 1278 cm<sup>-1</sup>. Bands of 1483 and 1275 cm<sup>-1</sup> were strongest in dark condition, followed by 1397 cm<sup>-1</sup>, while band at 1278 cm<sup>-1</sup> was strongest at UV irradiation, followed by 1479 and 1395 cm<sup>-1</sup>. This indicated that the main products under both different conditions were nitrate and sulfate species. Several new cross bands appeared in the asynchronous map under dark condition (Fig. 3c), and the sequential order for the band's changes analyzed (Table S6 in Supporting information) and shown in Scheme 1b. According to the results (Fig. 3d, Table S7 in Supporting information and Scheme 1b), bidentate sulfate was the first functional group to generated under UV. However, for the dark experiment, bidentate nitrate took the lead. To the final product, both in UV and dark experiments, monodentate nitrate was the final functional group. In this study, only one experiment (NO<sub>2</sub> and FOS in dark) final product was bidentate nitrate. It indicated SDS offered supplemental electron to  $\alpha$ -Fe<sub>2</sub>O<sub>3</sub> aerosol. With UV light or SO<sub>2</sub> injection, the microenvironment of FOS changed. Therefore, monodentate nitrate was the final generated for other experiments. These results suggested the nitrate species related to the oxidation status of reactants and reaction environment. The SDS offered oxidation capability from sulfate ion and SO<sub>2</sub> supplied its catalysis function. The long chain of SDS could change its adsorption status with UV irradiation and protected aerosols through its sacrificial characteristics. In other research, the surface active compounds could slow the reactive uptake of trace gases to aerosol [41]. In this study, SDS played two roles, *i.e.*, photoresist and acid catalysis.

In conclusion, we reinterpreted the reactions of NO<sub>2</sub> with or without SO<sub>2</sub> mixture gas on the surface of  $\alpha$ -Fe<sub>2</sub>O<sub>3</sub> particles with or without SDS by using 2D-COS. SDS changed the sequence order of nitrate and nitrite species during reactions. Monodentate nitrate was the final product of NO<sub>2</sub> and  $\alpha$ -Fe<sub>2</sub>O<sub>3</sub> in oxidation conditions. Bidentate nitrate was final formation only observed in the heterogeneous reaction of NO<sub>2</sub> and FOS without UV light. The functions of SDS were the catalysis and photoresist. The surface active compounds extended the environmental lifetime of heterogeneous

reactions between trace gases and aerosols. This study provided a new angle for reaction studies in environmental catalysis field.

### Declaration of competing interest

The authors declare that they have no known competing financial interests or personal relationships that could have appeared to influence the work reported in this paper.

### Acknowledgment

This work was supported by the National Natural Science Foundation of China (Nos. 41807304 and 22206130).

### Supplementary materials

Supplementary material associated with this article can be found, in the online version, at doi:10.1016/j.ccl.2023.109038.

### References

- [1] K.D. Perry, S.S. Cliff, M.P. Jimenez-Cruz, *J. Geophys. Res. Atmos.* 109 (2004), doi:10.1029/2004JD004979.
- [2] I. Tegen, A.A. Lacis, I. Fung, *Nature* 380 (1996) 419–422.
- [3] L.Y. Wu, S.R. Tong, L. Zhou, W.G. Wang, M.F. Ge, *J. Phys. Chem. A* 117 (2013) 3972–3979.
- [4] X. Zhao, L.D. Kong, Z.Y. Sun, et al., *J. Phys. Chem. A* 119 (2015) 4001–4008.
- [5] K. Hans Wedepohl, *Geochim. Cosmochim. Acta* 59 (1995) 1217–1232.
- [6] R.L. Siefert, S.O. Pehkonen, Y. Erel, M.R. Hoffmann, *Geochim. Cosmochim. Acta* 58 (1994) 3271–3279.
- [7] J. Baltrusaitis, D.M. Cwiertny, V.H. Grassian, *Phys. Chem. Chem. Phys.* 9 (2007) 5542.
- [8] K.J. Li, L.D. Kong, A. Zhanzakova, et al., *Environ. Sci. Nano* 6 (2019) 1838–1851.
- [9] Z.L. Huang, Z.H. Zhang, W.H. Kong, et al., *Atmos. Environ.* 166 (2017) 403–411.
- [10] R. Li, X.H. Jia, F. Wang, et al., *Chemosphere* 242 (2020) 125273.
- [11] H.B. Fu, X. Wang, H.B. Wu, Y. Yin, J.M. Chen, *J. Phys. Chem. C* 111 (2007) 6077–6085.
- [12] Q.X. Ma, Y.C. Liu, H. He, *J. Phys. Chem. A* 112 (2008) 6630–6635.
- [13] C.F. Pereira, C. Pasquini, *Quim. Nova* 29 (2006) 143–148.
- [14] I. Noda, *J. Mol. Struct.* 1069 (2014) 23–49.
- [15] Y. Park, I. Noda, Y.M. Jung, *J. Mol. Struct.* 1124 (2016) 11–28.
- [16] I. Noda, *Chin. Chem. Lett.* 26 (2015) 167–172.
- [17] P. Lasch, I. Noda, *Appl. Spectrosc.* 73 (2019) 359–379.
- [18] S.T. Mu, D.X. Sun, Y.X. Liu, et al., *J. Environ. Chem. Eng.* 10 (2022) 107158.
- [19] K.A. Wokosin, E.L. Schell, J.A. Faust, *Environ. Sci. Atmos.* 2 (2022) 775–828.
- [20] N. Sareen, A.N. Schwiier, T.L. Latham, A. Nenes, V.F. McNeill, *Proc. Natl. Acad. Sci. U. S. A.* 110 (2013) 2723–2728.
- [21] J.A. Faust, L.P. Dempsey, G.M. Nathanson, *J. Phys. Chem. B* 117 (2013) 12602–12612.
- [22] N.O.A. Kwamena, J. Buajarern, J.P. Reid, *J. Phys. Chem. A* 114 (2010) 5787–5795.
- [23] A. Norouzi, A. Nezamzadeh-Ejehieh, *Phys. B* 599 (2020) 412422.
- [24] K.I. Hadjiivanov, *Catal. Rev.* 42 (2000) 71–144.
- [25] C. Liu, Q.X. Ma, Y.C. Liu, J.Z. Ma, H. He, *Phys. Chem. Chem. Phys.* 14 (2012) 1668–1676.
- [26] G.M. Underwood, T.M. Miller, V.H. Grassian, *J. Phys. Chem. A* 103 (1999) 6184–6190.
- [27] L.Y. Wu, S.R. Tong, M.F. Ge, *J. Phys. Chem. A* 117 (2013) 4937–4944.
- [28] B.W. Chu, Y.L. Wang, W.W. Yang, et al., *Atmos. Chem. Phys.* 19 (2019) 14777–14790.
- [29] A.L. Goodman, E.T. Bernard, V.H. Grassian, *J. Phys. Chem. A* 105 (2001) 6443–6457.
- [30] Z.F. Zhang, J. Shang, T. Zhu, et al., *J. Environ. Sci.* 24 (2012) 1753–1758.
- [31] C. Wang, L.D. Kong, S.Y. Jin, et al., *Atmosphere* 13 (2022) 333–341.
- [32] H.J.Y. Niu, K.Z. Li, B.W. Chu, W.K. Su, J.H. Li, *Environ. Sci. Technol.* 51 (2017) 9596–9604.
- [33] J. Baltrusaitis, P.M. Jayaweera, V.H. Grassian, *Phys. Chem. Chem. Phys.* 11 (2009) 8295–8305.
- [34] B.C. Hixson, J.W. Jordan, E.L. Wagner, H.M. Bevsek, *J. Phys. Chem. A* 115 (2011) 13364–13369.
- [35] Y.F. Cheng, G.J. Zheng, C. Wei, et al., *Sci. Adv.* 2 (2016) e1601530.
- [36] N. Yang, N.T. Tsona, S.M. Cheng, et al., *Environ. Sci. Proc. Imp.* 22 (2020) 408–417.
- [37] S. Goryo, K. Iwata, *J. Phys. Chem. Lett.* 14 (2023) 1479–1484.
- [38] J.A. Faust, J.P.D. Abbatt, *J. Phys. Chem. A* 123 (2019) 2114–2124.
- [39] Z.Y. Sun, L.D. Kong, X. Zhao, et al., *J. Phys. Chem. A* 119 (2015) 9317–9324.
- [40] L.H. Han, J.S. Gui, X.H. Liu, et al., *Environ. Sci. Nano* 9 (2022) 2470–2487.
- [41] J.A. Thornton, J.P.D. Abbatt, *J. Phys. Chem. A* 44 (2005) 10004–10012.